A Proximity-Based Programmable DNA Nanoscale Assembly Line

Article *in* Nature · May 2010

DOI: 10.1038/nature09026 · Source: PubMed

4 authors:

Hongzhou gu
Fudan University
38 PUBLICATIONS **1,524** CITATIONS
SEE PROFILE

Jie Chao
Shanghai Institute of Applied Physics
123 PUBLICATIONS **5,011** CITATIONS
SEE PROFILE

Shou-Jun Xiao
Nanjing University
122 PUBLICATIONS **3,419** CITATIONS
SEE PROFILE

Nadrian C. Seeman
New York University
428 PUBLICATIONS **39,932** CITATIONS
SEE PROFILE

Vol 465|13 May 2010|doi:10.1038/nature09026

LETTERS

A proximity-based programmable DNA nanoscale assembly line

Hongzhou Gu[1], Jie Chao[2], Shou-Jun Xiao[2] & Nadrian C. Seeman[1]

Our ability to synthesize nanometre-scale chemical species, such as nanoparticles with desired shapes and compositions, offers the exciting prospect of generating new functional materials and devices by combining them in a controlled fashion into larger structures. Self-assembly can achieve this task efficiently, but may be subject to thermodynamic and kinetic limitations: reactants, intermediates and products may collide with each other throughout the assembly time course to produce non-target species instead of target species. An alternative approach to nanoscale assembly uses information-containing molecules such as DNA[1] to control interactions and thereby minimize unwanted cross-talk between different components. In principle, this method should allow the stepwise and programmed construction of target products by linking individually selected nanoscale components—much as an automobile is built on an assembly line. Here we demonstrate that a nanoscale assembly line can be realized by the judicious combination of three known DNA-based modules: a DNA origami[2] tile that provides a framework and track for the assembly process, cassettes containing three independently controlled two-state DNA machines that serve as programmable cargo-donating devices[3,4] and are attached[4,5] in series to the tile, and a DNA walker that can move on the track from device to device and collect cargo. As the walker traverses the pathway prescribed by the origami tile track, it sequentially encounters the three DNA devices, each of which can be independently switched between an 'ON' state, allowing its cargo to be transferred to the walker, and an 'OFF' state, in which no transfer occurs. We use three different types of gold nanoparticle species as cargo and show that the experimental system does indeed allow the controlled fabrication of the eight different products that can be obtained with three two-state devices.

In Fig. 1a, we sketch the three basic components of our molecular assembly line. The three two-state DNA machines each carry a different type of cargo: a 5-nm gold particle, a coupled pair of 5-nm particles and a 10-nm particle. In addition to the two-state devices, the cassettes contain a double DNA domain[6,7] for insertion into the origami and a robot arm that can position the cargoes into proximity with the walker if so programmed. (Full details of the origami design are provided in Supplementary Fig. 1, cassette sequences are given Supplementary Figs 2–4, and walker sequence and movement are shown in Supplementary Fig. 5.)

Previously described DNA walkers have been largely bipedal[8–11], whereas the walker used here is based on a tensegrity-triangle organization[12]. Fig. 2a shows the molecular structure that gives it three 'hands' and four 'feet', all consisting of single-stranded DNA segments. The hands accept and bind the cargo species that are appropriately placed for pick up. The feet bind to single strands on the origami surface and allow locomotion. To ensure that the walker is properly oriented towards the cargo sources, its fourth foot is bound at all stations where cargo is to be transferred. Each step of the walker entails a 120° rotation; two steps are needed to move the walker from one cargo-donating station to the next. All positional transitions of the walker and all cargo transfers from the arms of the cargo-bearing devices to the walker are performed using toehold-binding/branch-migration methods[13], for which both the cargoes and the two-state devices are endowed with appropriate DNA sequences. Figure 2b illustrates the mode of walking and Fig. 2c shows the proximity-based cargo attachment process for cassette one. (For non-denaturing gels of the cassettes and the walker, and non-denaturing gels of gold–DNA conjugates, see Supplementary Figs 6 and 7, respectively.)

The three DNA machines are independently programmed either to donate cargo or not, so the assembly line can produce eight distinct products. The example in Fig. 1 is for all machines donating cargo to the walker, with the 11 separate processing steps sketched in panel Fig. 1a. The state of the system on the right-hand side of Fig. 1a is visualized using AFM in Fig. 1b. (We note that the gold nanoparticle cargoes and the origami are the only features visible in the images, and that the nanoparticles attached to the walker are not individually resolved.) Steps 1, 5 and 9 respectively involve the transitions of the first, second and third two-state devices from the JX_2 (OFF) state to the PX (ON) state, which allows cargo donation; the actual transfers of the cargo particles to the walker respectively occur in steps 2, 6 and 10. Steps 3 and 7 involve the movement of the walker from a cargo-donating station to an intermediate position, and in steps 4 and 8 the walker completes its movement from the intermediate position to the next cargo-donating station. Step 11 removes the walker from the origami.

The motion of a cargo particle associated with switching its DNA device from the JX_2 state to the PX state, allowing particle transfer, is evident from the changes in the AFM images when going from state (i) to state (ii). The movement of the walker and the first cargo particle from the first particle-donating station to the second station is evident from the changes in the AFM images corresponding to states (ii) and (iii). The analogous changes involving the second particle-donating station can be seen in the transition from state (iii) to state (iv) (the second particle has been moved to the walker track) and in the transition from state (iv) to state (v) (the walker has moved its two cargoes to the third cargo-donating station). Finally, the changes in the AFM images corresponding to states (v) and (vi) show the addition of the third cargo to the walker. (For AFM images of the walker in all positions, including intermediate steps, see Supplementary Fig. 8.)

A key feature of the assembly line is the programmability of the cargo-donating DNA machines, which allows the generation of eight different products, as illustrated in Fig. 3a. The system can be preprogrammed to produce a desired product, or designated DNA machines can be switched dynamically from OFF to ON as the walker executes its trajectory (Supplementary Fig. 9.) Schematics of the final

[1]Department of Chemistry, New York University, New York, New York 10003, USA. [2]State Key Laboratory of Coordination Chemistry, School of Chemistry and Chemical Engineering, Nanjing National Laboratory of Microstructures, Nanjing University, Nanjing 210093, China.

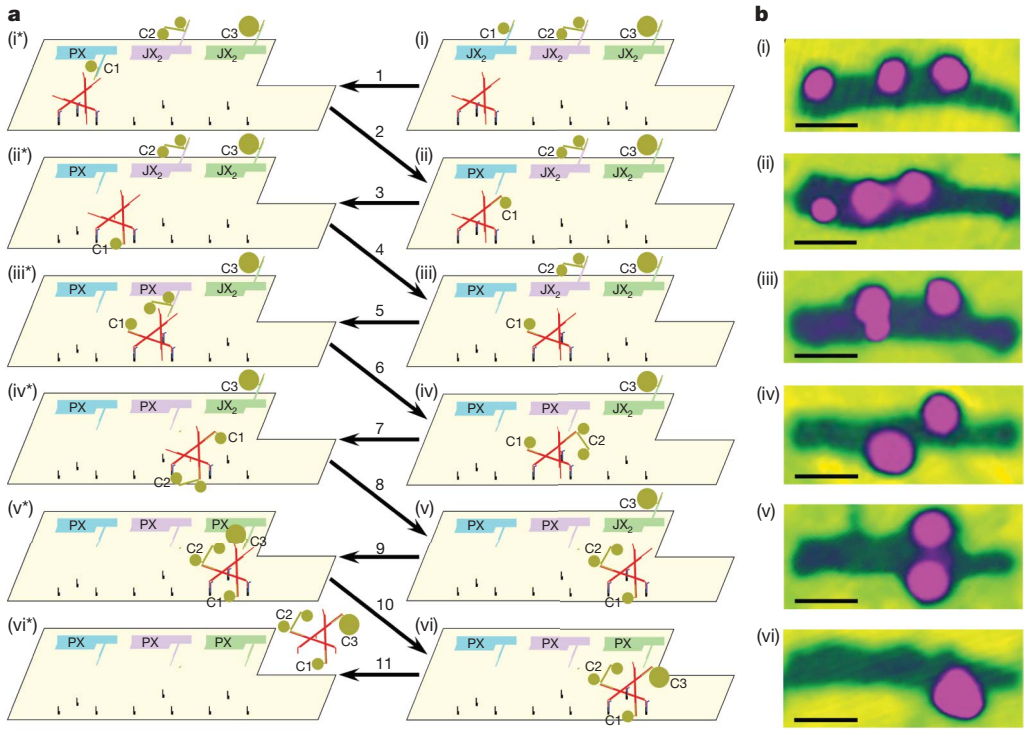

Figure 1 | The molecular assembly line and its operation. **a**, The basic components of the system are the origami tile (shown as a tan outline), programmable two-state DNA machines inserted in series into the file (shown in blue, purple and green) and the walker (shown as a trigonal arrangement of DNA double helices in red). The machines have cargoes consisting respectively of a 5-nm gold particle (C1), a coupled pair of 5-nm particles (C2) and a 10-nm particle (C3) (indicated by green–brown dots), and their state can be PX (meaning ON or 'donate' cargo) or JX_2 (meaning OFF or 'do not donate' cargo). In the example shown, the walker collects cargo from each machine. **b**, Atomic force micrographs of the system corresponding to the process steps sketched as states (i)–(vi) in **a**. Atomic force microscopy (AFM) was performed by tapping in air; this mode of AFM results in only the nanoparticles and the origami being visible, and the individual nanoparticle components are not individually resolved. Owing to the washing procedures between steps, the AFM images are not of the same individual assembly line. Scale bars, 50 nm.

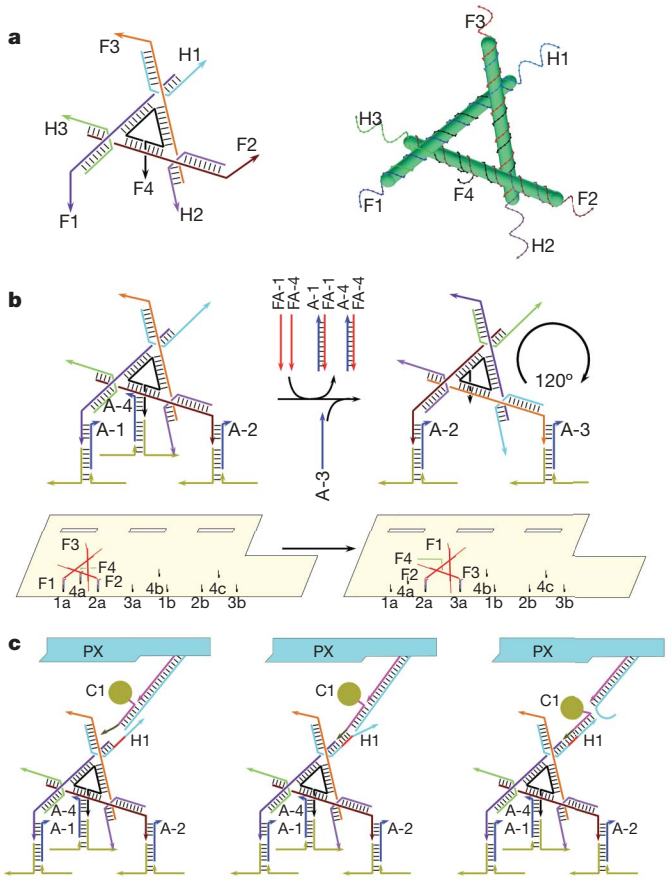

state of the system, with the eight possible products on the origami tiles, are shown in Fig. 3b, and Fig. 3c shows the corresponding transmission electron microscope images. The images clearly illustrate that all assembly pathways function, with programming of the DNA machines as (JX_2, JX_2, JX_2) giving the null product (state (i)), whereas programming as (PX, JX_2, JX_2), (JX_2, PX, JX_2) or (JX_2, JX_2, PX) adds cargo to the walker at the first, second or third station (state (ii), (iii) or (iv), respectively). When the DNA machines are programmed as (PX, PX, JX_2), (PX, JX_2, PX) or (JX_2, PX, PX), cargo is added to the walker twice, such that it contains the 5-nm particle plus the coupled particles, the 5-nm particle plus the 10-nm particle, or the coupled particles plus the 10-nm particle (state (v), (vi) or (vii), respectively). If the system is in the state (PX, PX, PX) (state (viii)), the walker collects cargo at all three stations, as shown in Fig. 1.

The yield of the assembly process depends directly on the number of additions that are made to the walker. For the triple addition, we obtain a yield of 43%, or an average step yield of ~75%; the failure products are 20% double-addition products and 37% single-addition products. For double additions, the yield is ~70%; for example, for the 5-nm/10-nm double product we obtain a 72% yield (step yield, ~85%), with 2%

Figure 2 | Details of the walker, movement and cargo transfer. **a**, Walker structure. The drawing on the left is a stick figure indicating the three hands (H1–H3) and four feet (F1–F4). The image on the right shows the strand structure. **b**, Movement. Walker reactions are shown in the upper two images, and movement on the origami is shown in the lower two images. A-*k* binds F*k* to the origami and FA-*k* is a fuel strand that removes A-*k*, undoing the corresponding binding. Foot-binding sites on the origami are labelled such that in its *n*th binding to the origami, F*k* binds to site *kn*. Supplementary Fig. 5 shows the complete walker transit. **c**, Cargo transfer. The PX state brings the arm of cassette one close to H1 (left), the brown toehold binds its complement (red; centre) and branch migration transfers the cargo strand to H1 (right).

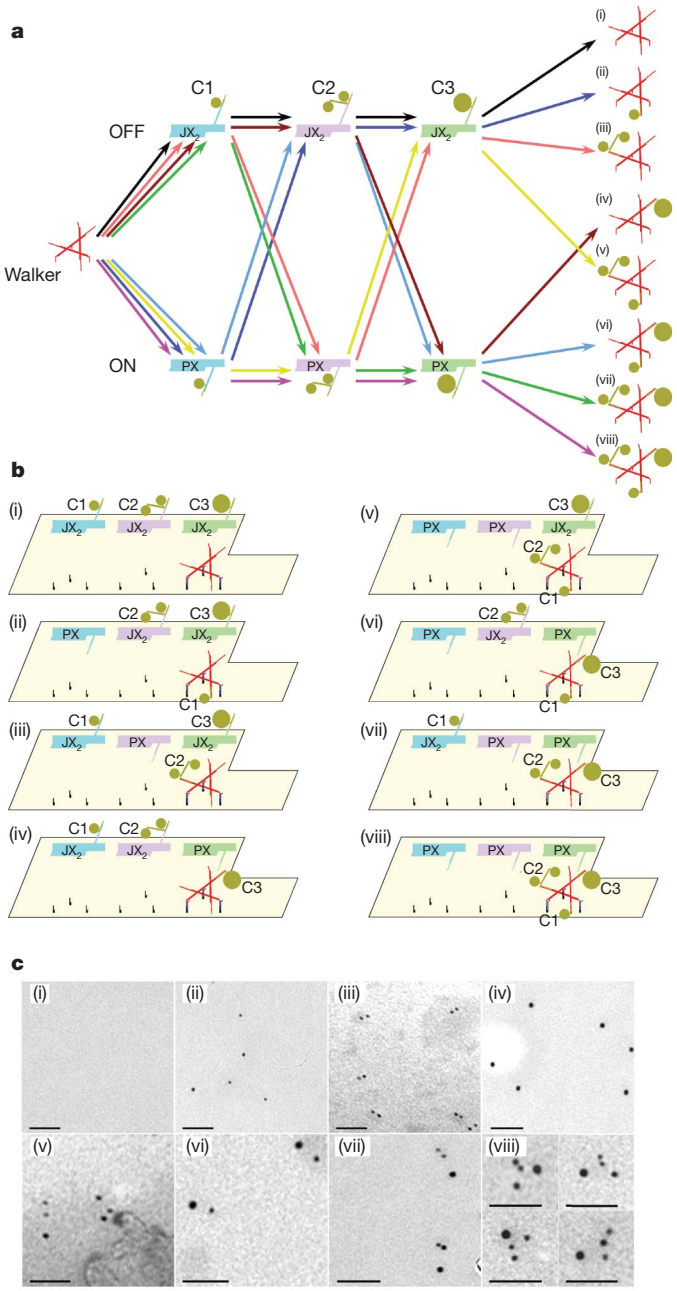

Figure 3 | The eight products of the assembly line. Roman numerals indicate the different pathways illustrated. **a**, The eight possible products that can be generated through appropriate programming of the states of the three DNA machines. The walker is shown on the left, without cargo. Each DNA machine is shown twice: in the upper row in the OFF state, in which no cargo transfer takes place, and in the lower row in the ON state, in which cargo can be transferred to the walker. The different assembly trajectories are colour-coded as black (i), dark blue (ii), rose (iii), brown (iv), yellow/green (v), light blue (vi), green (vii) and purple (viii), giving the respective products shown on the right. **b**, Schematics of the final state the system reaches for each of the eight assembly pathways. The states of the cassettes and the dispositions of the cargo species (attached to the robot arms or attached to the walker) are shown. **c**, Transmission electron microscope images of the products generated in each of the assembly pathways. (Note that transmission electron microscopy resolves the individual gold nanoparticles.) In each image, several products generated by the given pathway are visible. Scale bars, 50 nm.

incorrect products and 26% single-addition products. Programmed single products are obtained at >90%, with an error rate of ~1%. The low level of incorrect products (as opposed to failure products) suggests that there is no addition to the walker from the OFF state, and that the assembly lines work intramolecularly and with minimal cross-talk between different assembly lines present in the reaction medium. Thus, the strategy adopted here to sequester reactants has proved successful. The decrease in step yield for more complex products suggests that there may be steric interference between individually added components, possibly owing to the small size of the walker (which is necessitated by the limited size of the origami tile we have used). The structural integrity of the tensegrity-triangle walker seems unlikely to be a problem, as it seems to be quite good: the estimated separation between the 5-nm particle and the 10-nm particle is 27.5 ± 13 nm, and the observed separation is 25.9 ± 7.3 nm. (See Supplementary Figs 10–12 and Supplementary Table 1 for sampling images and statistical details.)

Numerous writers on nanotechnology have commented on the possibility of building assembly lines on the nanometre and chemical scales (1–2 Å), analogous to those used on the macroscopic scale[14,15]. The basic operation of such assembly lines would differ from that of their macroscopic counterparts because different forces and effects dominate at the different scales, but the basic notion is still that it might be possible to build products difficult to produce by more conventional techniques. We have shown in this work that it is possible to use nanometre-scale DNA devices to put together, in a controlled fashion, a series of complex non-covalent constructs with acceptable yields. Furthermore, although we have not yet tried reloading the device for a second round of construction, there are no fundamental obstacles to taking this step in our non-covalent system. In closing, we note that DNA has been used to promote chemical reactions between attached moieties via proximity (see, for example, ref. 16); our system adds elements of both programmability and temporal control to DNA-assisted assembly and might therefore, with some alterations, even allow the construction of new chemical species that are not readily synthesized by other means.

METHODS SUMMARY

We designed DNA strands using SEQUIN[17], synthesized them using routine phosphoramidite chemistry[18], and gel purified them. Hydrogen-bonded DNA devices were formed from stoichiometric mixtures of the strands and were cooled from 70 °C to room temperature (21 °C). DNA origami tiles were formed by combining staple strands and 5 µl of 30 nM (equivalent to 0.15 pmol) single-stranded M13 genomic DNA (New England Biolabs) in a 7:1 ratio; the system was cooled from 90 °C to 60 °C on a thermocycling machine over 30 min, and then cooled further to 16 °C over 90 min. The procedure of ref. 19 was used to remove excess helper strands from the origami solution. The origami tiles were purified using a Microcon centrifugal filter device (molecular weight cut-off, 50,000; Millipore). We adjusted the final concentration of the origami tiles to 1 nM, estimated by $A_{260\,nm}$. The three cassettes and the walker were added to the origami by mixing 200 µl of a solution containing 1 nM origami tiles with 4 µl each of 50 nM solutions containing the cassettes and the walker. Walking was done by releasing the left foot of the walker using unset (fuel) strands, by treating for 2 h at room temperature; strands corresponding to the new position were added and equilibrated for another 2 h. To switch the state of a cassette in the origami, it was treated for 2 h with unset-strand solutions to ~1 nM, and this was followed by addition of the set strands for 6 h. Nanoparticles were prepared conjugated with a single strand of DNA by methods described previously[20,21]. We used standard methods for transmission electron microscopy, tapping-mode AFM in buffer, tapping-mode AFM in air, gel electrophoresis and elution.

Full Methods and any associated references are available in the online version of the paper at www.nature.com/nature.

Received 30 October 2009; accepted 12 February 2010.

1. Seeman, N. C. & Lukeman, P. S. Nucleic acid nanostructures. *Rep. Prog. Phys.* **68**, 237–270 (2005).
2. Rothemund, P. W. K. Scaffolded DNA origami for nanoscale shapes and patterns. *Nature* **440**, 297–302 (2006).
3. Yan, H., Zhang, X., Shen, Z. & Seeman, N. C. A robust DNA mechanical device controlled by hybridization topology. *Nature* **415**, 62–65 (2002).
4. Ding, B. & Seeman, N. C. Operation of a DNA robot arm inserted into a 2D DNA crystalline substrate. *Science* **314**, 1583–1585 (2006).
5. Gu, H., Chao, J., Xiao, S. J. & Seeman, N. C. Dynamic patterning programmed by DNA tiles captured on a DNA origami substrate. *Nature Nanotechnol.* **4**, 245–249 (2009).

6. Ding, B., Sha, R. & Seeman, N. C. Pseudohexagonal 2D DNA crystals from double crossover cohesion. *J. Am. Chem. Soc.* **126,** 10230–10231 (2004).
7. Constantinou, P. E. *et al.* Double cohesion in structural DNA nanotechnology. *Org. Biomol. Chem.* **4,** 3414–3419 (2006).
8. Sherman, W. B. & Seeman, N. C. A precisely controlled DNA bipedal walking device. *Nano Lett.* **4,** 1203–1207 (2004).
9. Shin, J. S. & Pierce, N. A. A synthetic DNA walker for molecular transport. *J. Am. Chem. Soc.* **126,** 10834–10835 (2004).
10. Bath, J. Green, S. J., Allen, K. E. & Turberfield, A. J. Mechanism for a directional, processive and reversible DNA walker. *Small* **5,** 1513–1516 (2009).
11. Omabegho, T., Sha, R. & Seeman, N. C. A bipedal DNA Brownian motor with coordinated legs. *Science* **324,** 67–71 (2009).
12. Liu, D., Wang, W., Deng, Z., Walulu, R. & Mao, C. Tensegrity: construction of rigid DNA triangles with flexible four-arm junctions. *J. Am. Chem. Soc.* **126,** 2324–2325 (2004).
13. Yurke, B., Turberfield, A. J., Mills, A. P. Jr, Simmel, F. C. & Newmann, J. L. A DNA-fuelled molecular machine made of DNA. *Nature* **406,** 605–608 (2000).
14. Drexler, K. E. Machine-phase nanotechnology. *Sci. Am.* **285,** 74–75 (2001).
15. Smalley, R. E. Of chemistry, love and nanobots. *Sci. Am.* **285,** 76–77 (2001).
16. Gartner, Z. J., Kanan, M. W. & Liu, D. R. Multi-step small molecule synthesis programmed by DNA templates. *J. Am. Chem. Soc.* **124,** 10304–10306 (2002).
17. Seeman, N. C. *De novo* design of sequences for nucleic acid structure engineering. *J. Biomol. Struct. Dyn.* **8,** 573–581 (1990).
18. Caruthers, M. H. Gene synthesis machines: DNA chemistry and its uses. *Science* **230,** 281–285 (1985).
19. Ke, Y. Lindsay, S. Chang, Y., Liu, Y. & Yan, H. Self-assembled water-soluble nucleic acid probe tiles for label-free RNA hybridization assays. *Science* **319,** 180–183 (2008).
20. Zheng, J. *et al.* Two-dimensional nanoparticle arrays show the organizational power of robust DNA motifs. *Nano Lett.* **6,** 1502–1504 (2006).
21. Alivisatos, A. P. *et al.* Organization of 'nanocrystal molecules' using DNA. *Nature* **382,** 609–611 (1996).

Supplementary Information is linked to the online version of the paper at www.nature.com/nature.

Acknowledgements We are grateful to J. Canary, H. Yan, C. Mao and R. Sha for comments on this manuscript. This research has been supported by the following grants: GM-29544 from the US National Institute of General Medical Sciences, CTS-0608889 and CCF-0726378 from the US National Science Foundation, 48681-EL and W911NF-07-1-0439 from the US Army Research Office, N000140910181 and N000140911118 from the US Office of Naval Research and a grant from the W. M. Keck Foundation (to N.C.S.); and 2007CB925101 from the National Basic Research Program of China and 20721002 from the National Natural Science Foundation of China (to S.-J.X.). H.G. thanks New York University for a Dissertation Fellowship and J.C. thanks the Chinese Scholarship Council for a research fellowship.

Author Contributions H.G. and J.C. did the research, analysed data and wrote the paper. S.-J.X. analysed data and wrote the paper. N.C.S. designed the project, analysed data and wrote the paper.

Author Information Reprints and permissions information is available at www.nature.com/reprints. The authors declare no competing financial interests. Readers are welcome to comment on the online version of this article at www.nature.com/nature. Correspondence and requests for materials should be addressed to N.C.S. (ned.seeman@nyu.edu).

METHODS

Design, synthesis and purification of DNA. Strands for the cassettes and walker molecules were designed using the program SEQUIN[17]. Oligonucleotides were synthesized on an Applied Biosystems 394 synthesizer using routine phosphoramidite chemistry, or were purchased from Integrated DNA Technologies. DNA strands were purified by gel electrophoresis: bands were cut out of 10–20% denaturing gels and eluted in a solution containing 500 mM ammonium acetate, 10 mM magnesium acetate and 1 mM EDTA.

Formation of hydrogen-bonded DNA devices. Stoichiometric mixtures of the strands (estimated by $A_{260\,nm}$) were prepared separately for each molecule at a concentration of 50 nM in a solution containing 40 mM Tris-HCl (pH 8.0), 20 mM acetic acid, 2.5 mM EDTA and 12.5 mM magnesium acetate. The unmodified cargo strands were replaced by 1:1 gold–DNA conjugates for each cassette and those cargo strands on the cassettes were protected by shield strands. The mixture was cooled from 70 °C to room temperature (21 °C) in a 1-l water bath over 24 h.

Formation of the DNA origami tiles. Single-stranded M13 genomic DNA (5 μl, 30 nM (equivalent to 0.15 pmol); New England Biolabs) was combined with the staple strands (1:7 molar ratio of plasmid to staple strands, 1:2 molar ratio of plasmid to purified staple strands with extensions) and added to a buffer solution containing 40 mM Tris-HCl (pH 8.0), 20 mM acetic acid, 2.5 mM EDTA and 12.5 mM magnesium acetate. The final volume of the system was 100 μl. The system was cooled from 90 °C to 60 °C on a thermocycling machine over 30 min, and then cooled further to 16 °C over 90 min. The concentration of the DNA origami at this stage was 1.5 nM. Insofar as could be estimated by AFM, the yield was virtually quantitative.

Preparation of gold–DNA conjugates with discrete copies of DNA. Bis(*p*-sulphonatophenyl)phenylphosphine dehydrate dipotassium salt (40 mg; BSPP, Strem Chemicals) was mixed with 100 ml citrate-ion-stabilized gold nanoparticles (Ted Pella) and the mixture was stirred overnight for ligand exchange. Phosphine ligands lead to enhanced stability against higher electrolyte concentrations. The mixture was concentrated up to the micromolar range after phosphine coating, as determined by measuring the optical absorbance at a wavelength of 520 nm. Gold–DNA conjugates were prepared by mixing gold nanoparticles with 5′-end-thiolated (-SH) single-stranded DNA (ssDNA) (complementary strands were added to increase the DNA size if the strands were shorter than 50 bases) in a molar ratio of 1:1, and incubated in ×0.5 TBE buffer (89 mM Tris, 89 mM boric acid, 2 mM EDTA, pH 8.0) containing 50 mM NaCl overnight at room temperature. Gold–DNA conjugates carrying discrete numbers of copies of DNA strands were separated using 3% agarose gel (running buffer, ×0.5 TBE; loading buffer, 50% glycerol; 15 V cm^{-1}). The desired band, containing a 1:1 ratio of gold–DNA conjugates with a single DNA strand, was collected and electroeluted into a pocket of dialysis membrane (molecular weight cut-off (MWCO), 10,000). Gold–DNA conjugates were recovered using a Microcon centrifugal filter device (MWCO, 50,000; Millipore) and quantified using optical absorbance at 520 nm. The 1:1 gold–DNA conjugates were further stabilized with short thiolated (-SH) oligonucleotides T_5-ssDNA ($[HS\text{-}T_5]/[Au] = 30$, in ×0.5 TBE and 50 mM NaCl) and incubated overnight at room temperature. Short DNA components provide additional stability against the higher electrolyte concentrations necessary for DNA self-assembly. Gold–DNA conjugates with differently sized gold nanoparticles were prepared using the same method.

Purification of the DNA origami. The procedure of ref. 19 was used to remove excess helper strands from the origami solution. The origami tiles were purified with a Microcon centrifugal filter device (MWCO, 50,000; Millipore). We adjusted the final concentration of the origami tiles to 1 nM, estimated by $A_{260\,nm}$.

Placing the three cassettes and the walker onto the DNA origami. A solution (200 μl) containing 1 nM origami tiles was mixed with 4 μl each of 50 nM solutions containing cassettes one, two and three and the walker (with the anchor strands that would position the walker at the first transfer station, near cassette one, the starting point of the pathway). The system was heated to 40 °C and slowly cooled to 4 °C over 1 day in a 2-l water bath. The final solution contained 0.2 pmol of each of the five components in a 1:1:1:1:1 molar ratio. All cargo strands on the cassettes were protected by the shield strands, which means that no addition of cargo to the walker could happen during this process. Insofar as could be estimated by AFM, the yield of capturing one cassette was virtually quantitative and the yield of capturing all three cassettes was around 80–90%.

Walking and assembling. The shield strands were removed by adding equimolar quantities of fuel strands (which are complementary to the entire lengths of the shield strands, including their toeholds) at room temperature for 2 h before starting the walk. The cassettes were all set to the default JX_2 state at the beginning. To perform the assembly line with different kinds of cargo addition to the walker, the cassettes were pre-programmed to the desired state before binding to the origami or were dynamically switched to the desired state during the walking process. Both procedures have been performed and the two methods generated the same results (see transmission electron microscopy (TEM) images). The left foot of the walker was released by mixing equimolar quantities of fuel strands (complementary to the entire length of the anchor strands) at room temperature for 2 h to remove its anchor strands. Equimolar quantities of new anchor strands were added and mixed at room temperature for another 2 h to rotate the walker by 120°, and moved the walker one step forward by anchoring the third foot with the corresponding extension of the origami helper strand. This was repeated four times until the walker walked four steps to the end of the pathway. Anchor strands for the fourth foot were added to position the walker body close to the cassette whenever the walker passed by the transfer station near the cassette.

Operation of cassettes on the origami. The JX_2 state (OFF state) was the default state when the three cassettes were inserted into the origami, so the system was initiated in the state (JX_2, JX_2, JX_2). To switch to a different conformation, for example (JX_2, JX_2, PX), 4 μl each of 50 nM solutions containing strands Fuel-J1 and Fuel-J2 for cassette three were added to the 216-μl solution containing a 1:1:1:1:1 ratio of origami, cassette one, cassette two, cassette three and the walker, each at a concentration of ~1 nM. The solution was stirred with a pipette for 5 min and left at room temperature for 2 h. Then 4 μl each of 50 nM solutions containing the Set-P1 and Set-P2 strands for cassette three were added to the solution. The solution was stirred again with a pipette for 5 min and kept at room temperature for 6 h to establish the new (JX_2, JX_2, PX) conformation. The two different ways of setting the conformation of the system, that is, pre-programming the cassettes before binding to the origami or inserting the cassettes in a default state into the origami and then reprogramming, produced the same results.

Elution of the walker out of the origami for TEM. After the walker arrived at the end of the pathway and all the additions of cargo had been accomplished, the mixture was first treated with the shield strands of the three cassettes for 2 h to protect the untransferred cargoes, and then treated with the walker fuel strands for 2 h to remove the anchor strands and release the walker from the origami. The mixture was then treated with biotin-modified anchor strands (complementary with the extension part of strand seven of the walker) at room temperature for 2 h, and then treated with magnetic streptavidin beads at room temperature for 45 min. After this, the tube with the mixture solution was put on a magnetic stand for another 45 min to allow the beads with the walkers to gather at the bottom. The supernatant liquid was discarded and fuel strands (completely complementary with the biotin-modified anchor strands) were added to the tube to release the walker from the beads. The tube was then again put on a magnetic stand for 45 min to allow only the beads to gather at the bottom. The supernatant liquid (the walker) was transferred to another tube for TEM.

Non-denaturing polyacrylamide gel electrophoresis. Non-denaturing gels consisted of 5% acrylamide (19:1, acrylamide: bisacrylamide) and the running buffer consisted of 40 mM Tris-HCl (pH 8.0), 20 mM acetate acid, 2 mM EDTA and 12.5 mM magnesium acetate (×1 TAE Mg^{-1}). Tracking dye containing ×1 TAE Mg^{-1}, 50% glycerol and 0.02% each of bromophenol blue and xylene cyanol FF was added to the sample buffer. Gels were run on a Hoefer SE 600 gel electrophoresis unit at 4 V cm^{-1} at 4 °C, and were stained with 0.01% Stains-all dye (Sigma) in 45% formamide.

AFM imaging by tapping in buffer. A 5-μl sample was spotted on freshly cleaved mica (Ted Pella), and the sample was left to adsorb for 2 min. Additional fresh ×1 TAE Mg^{-1} (12.5 mM) buffer was added to both the mica and to the liquid cell. The AFM imaging was performed on a NanoScope IV (Digital Instruments) in buffer in tapping mode, using commercial cantilevers with Si_3N_4 tips (Veeco) for buffer mode.

AFM imaging by tapping in air. A 5-μl sample was spotted on freshly cleaved mica, and the sample was left to adsorb for 1 min. The excess sample was wicked out from the mica with a piece of filter paper. The mica was washed with double-distilled water three times by loading 30 μl H_2O on it and wicking out the excess with filter paper. Then the mica was dried in air while covered by a Petri dish. The AFM imaging was performed on a NanoScope IV (Digital Instruments) in air in tapping mode, using commercial cantilevers with Si tips for air mode.

TEM analysis. The TEM sample was prepared by dipping the carbon-coated grid (400 mesh, Ted Pella) into DNA tubes for 30 s. The grid was then taken out and excess liquid was wicked out with filter paper. The grid was then placed on filter paper and covered with a Petri dish to dry. TEM images were collected using a JEOL 1200 EXII electron microscope (Peabody) operated at 60 kV.